

Accepted Manuscript

Title: Nanoindentation of functionally graded hybrid polymer/metal thin films

Author: J. Nunes A.P. Piedade

PII: S0169-4332(13)01487-6
DOI: <http://dx.doi.org/doi:10.1016/j.apsusc.2013.08.009>
Reference: APSUSC 26150

To appear in: *APSUSC*

Received date: 12-6-2013
Revised date: 31-7-2013
Accepted date: 1-8-2013



Please cite this article as: J. Nunes, A.P. Piedade, Nanoindentation of functionally graded hybrid polymer/metal thin films, *Applied Surface Science* (2013), <http://dx.doi.org/10.1016/j.apsusc.2013.08.009>

This is a PDF file of an unedited manuscript that has been accepted for publication. As a service to our customers we are providing this early version of the manuscript. The manuscript will undergo copyediting, typesetting, and review of the resulting proof before it is published in its final form. Please note that during the production process errors may be discovered which could affect the content, and all legal disclaimers that apply to the journal pertain.

Nanoindentation of functionally graded hybrid polymer/metal thin films

J. Nunes and A. P. Piedade*

corresponding author: telef:+351239790700; fax:+351239790701; e-mail:
ana.piedade@dem.uc.pt

GNM-CEMUC – Department of Mechanical Engineering, University of Coimbra, Rua Luís Reis Santos, 3030-788 Coimbra, Portugal

Abstract

Hybrid functionally graded coatings (2D-FGC) were deposited by magnetron co-sputtering from poly(tetrafluoroethylene) (PTFE) and AISI 316L stainless steel (316L) targets. The carbon and fluorine content varied from 7.3 to 23.7 at.% and from 0 to 57 at.%, respectively. The surface modification was developed to change the surface of 316L vascular stents in order to improve the biocompatibility of the outmost layer of the metallic biomaterial. In-depth XPS analysis revealed the presence of a graded chemical composition accompanied by the variation of the film structure. These results were complemented by those of transmission electron microscopy (TEM) analysis that highlighted the nanocomposite nature of the coatings.

The nanomechanical characterization of 2D-FGC was performed by nanoindentation at several loads on the thin films deposited onto two different steel substrates: 316L and AISI M2. The study allowed establishing 0.7 mN as the load that characterized the coatings without substrate influence. Both hardness and Young modulus decrease with the increase of fluorine content due to the evolution in chemical composition, chemical bonds and structure.

Keywords: Functionally graded coating; Stents; Nanocomposite; Hybrid polymer/metal; Nanoindentation.

1. Introduction

Functional graded materials (FGM) are defined as engineered materials that present gradual transitions in microstructure and/or chemical composition [1,2]. Abrupt transitions in material properties induce undesirable stress concentrations that can compromise structural performance. In nature, these problems are controlled by gradually varying the material behavior through a structure, i.e, by developing functional graded materials.

This approach is appropriate when coating a bulk material with a thin film in order to increase the mechanical and chemical compatibility between coating and substrate. The authors have used the bio-inspired approach to deposited functional graded coatings (2D-FGC) from poly(tetrafluoroethylene) (PTFE) and AISI 316L stainless steel (316L) onto 316L vascular stents [3,4]. The aim was to improve biocompatibility of stents with a polymeric outmost layer, which was confirmed by preliminary *in vitro* tests [5], combined with mechanical resistance to withstand the stent expansion upon deployment, but without creating interface stresses between the coating and the thin film. In the published work the mechanical properties were evaluated by micro-hardness. However, for 2D-FGC with thickness varying from 400 to 700 nm the use of nanoindentation would constitute a more valid approach.

The first paper related with nanoindentation dates from 1990, where the authors determined the hardness and Young modulus of (Ti, Al)N and (Ti, Nb)N coatings. Even then the researchers were aware that some post indentation corrections were needed [6]. In fact, one of the problems associated with the evaluation of hardness in thin films is the integration of the substrate values in the indentation results. Some researchers analyzed, by transmission electron microscopy, the influence of the indentation at several loads on the cross-section of a TiN thin film deposited in different substrates. However, they could not identify the maximum load that only integrated the contribution of the coating for all substrates [7]. A

theoretical approach with some mathematical models was also developed for coated surfaces, but they are not unanimous accepted [8-11].

Furthermore, the current demanding for miniaturization of mechanical components led to a new emphasis of their analysis, for which nanoindentation is a powerful tool. The evaluation of the mechanical properties of silver or metallic glass nanowires, or even copper oxide nanocubes demonstrates the degree of accuracy of this technique [12,13]. Also, the use of this technique for the mechanical characterization of nanocomposites sputtered thin films is an usual approach, regardless of the technique used to deposit the coatings[14-16].

The use of nanoindentation for the characterization of functional graded thin films is exploited for several applications such as protection against metal dusting [17], high speed cutting tools [18] or protection of martensic steel for reactors [19]. However, it was not possible to find any work concerning the nanomechanical characterization of functionally graded coatings for biomedical applications although many studies concerning the use of nanoindentation on the characterization of functionally graded biological materials such as bone [20,21] and dental enamel and dentin [22,23] have been published.

Thus, the used of nanoindentation to mechanically characterize 2D-FGC for biomedical applications with less than 1 μm of thickness, with a nanocomposite structure, and with a progressively shifting chemical composition from the interface film/substrate up to the outmost layer, is a challenging study. The difficulty is enhanced when one of the materials that constitute the thin film is the same as the substrate. In this paper we wish to report a procedure to characterize the mechanical behavior of 2D-FGC by nanoindentation. Briefly, several tests were made, with different loads on the same film which was deposited on two different steel substrates. When both hardness and Young modulus converged to similar values, it was possible to evaluate the mechanical properties of the thin films without substrate influence.

2. Materials and methods

2.1. Deposition technique

Functionally graded thin films (2D-FGC) were deposited using a radiofrequency (r.f.) power supply of 1000 and 500W, branched to the two assisted magnetron targets and substrate holder, respectively. 316L stainless steel and PTFE targets with 100 mm in diameter were used. The parameters used in the deposition were: 10^{-4} Pa ultimate vacuum pressure; 5.1 W cm^{-2} discharge power densities for 316L target and from 0 to 1.3 W. cm^{-2} for PTFE target; 0.7 Pa total discharge pressure; and 15 min deposition time. The thin films were deposited onto glass lamellae ($R_a = 0.002 \mu\text{m}$), 316L stainless steel $10 \times 10 \text{mm}^2$ and 12mm of diameter AISI M2 steel substrates. The metallic material was polished with SiC paper grit down to 4000 mesh and with 1- μm -grain-size diamond paste to $R_a = 0.02 \mu\text{m}$. The substrate holder was placed directly over the 316L target in order to allow the sputtered steel to directly form the first layers of the coating due to the retarded arrival of the species sputtered from PTFE target.

2.2. Characterization techniques

The XPS analyses were performed in a VG-ESCLAB 250iXL spectrometer. The pressure in the analysis chamber was kept below 5×10^{-8} Pa and the analysis were performed using monochromatic radiation Al-K α ($h\nu = 1486.92$ eV). The photoelectrons were collected with an angle of 90° with respect to the surface of samples. The energy step was of 20 eV for the survey spectra and of 0.05 eV for the high-resolution spectra. The XPS was also used for the in-depth analysis of the thin films. The chemical compositions were obtained using the sensitivity factor of the Scofield library.

TEM analyses were performed on a Tecnai G2 microscope. The samples were cutted from a coated 316L AISI stainless steel thin foil with 0.1mm thickness, electro-eroded and finally thinned by ion milling in a Gatan Duo Ion Mill 600DIF.

Adhesion of the thin films to the AISI M2 steel substrate was evaluated by scratch test which was performed with a CSEM – REVETEST with an increment of $10 \text{ N}\cdot\text{s}^{-1}$ and a limit load of 70 N.

Nanoindentation was performed using the Micro Materials NanoTest system, in the load control mode. Several loads (40, 20, 15, 10, 5, 1.5, 0.75 and 0.30 mN) were applied on the thin film deposited on two different substrates: AISI M2 Steel and AISI 316L stainless steel. The method for obtaining the hardness and Young modulus from the loading/unloading curves has already been described elsewhere [24,25]. The load rate was tuned so that each test would last about 30 s, with 5 s hold period at the maximum load and 30 s hold period, during unloading, at 10% of the maximum load, for thermal drift correction. A minimum of 20 indentations were performed at each maximum load, using a Berkovich indenter. The β factor used was 1.034 and the area function $\text{Area} = A + B \cdot hc + C \cdot hc^2$ where A, B and C are variables which were calculated from the calibration tests with a fused silica standard, with a hardness of 8.8 GPa, and a Young modulus of 72 GPa.

3. Results and discussion

The chemical composition, thickness and designation of the deposited 2D-FGC are summarized in Table I. The results show that the increase of power density on the PTFE target induced the augmentation of carbon and fluorine content, although the C/F ratio decreased from 1.7 to 0.2. This fact is explained by the Gibbs' free energy values ($\Delta_f G^0$, in $\text{kJ}\cdot\text{mol}^{-1}$) for the formation of the metallic fluorides ($\Delta_f G^0 (\text{FeF}_2) = -668$; $\Delta_f G^0 (\text{NiF}_2) = -604$;

$\Delta_f G^0$ (CrF_3) = -1088) which are thermodynamically more favorable than the carbides formation ($\Delta_f G^0$ (Cr_7C_3) = -177; $\Delta_f G^0$ (Fe_3C) = +20) [26,27]. By increasing the power density on the PTFE target more C and F are ejected and available for the formation of the compounds. With the increase uptake of F for the formation of the metallic fluorides more carbon is left unreacted and is, probably, evacuated by the pumping system of the deposition equipment.

The in-depth XPS analysis of the samples demonstrated a chemical composition gradient through the thickness of the films, as exemplified in Figure 1 for Fe survey of sample F4. After peak deconvolution, the in-depth analysis also revealed that due to the continuous variation of the chemical composition the phasic composition also presents a gradient through the thickness of the coating, as previously described [3].

TEM analysis revealed that all thin films, with the exception of F6 and F7, present a nanocomposite structure as exemplified in Figure 2. The combination of the XPS results with TEM structural analysis allowed establishing a relation between the main compounds and the fluorine content of each thin film (Figure 3). The compounds present in all the 2D-FGC, although with varying concentrations, are iron carbide and iron and chromium difluorides. The chromium carbides content decrease from F0 to F4 and was not detected for samples with higher fluorine content. In these latest, the presence of the metallic fluorides NiF_2 , FeF_3 and CrF_3 along with graphitic carbon induces changes in the properties of the thin films. In fact, the adhesion of 2D-FGC to M2 substrates highlights this fact: only the samples with low fluorine content present cohesion failures (Lc1) although the same group of samples present the higher values of adhesion to the substrate, Lc2 >70N (Table II and Figure 4). As pointed out by some authors the quantitative adhesion measurement is a complex process even for a single monolithic coating [28], consequently the difficulty for the understanding the behavior of functional graded thin film increases. For F0 coating high values of Lc2 were expected due

to the chemical compatibility of a steel thin film deposited onto a steel substrate. For the lower fluorine contents (F1 and F2) it seems that the introduction of the new chemical elements, with the formation of a nanocomposite structure and the presence of new chemical compounds, induces a very strong cohesion of the thin film at the expenses of lowering the coating/substrate deformation resistance and, consequently, the Lc_2 value. The optimal compromise between these two apparent contradictory factors occurs for the thin film with 8.8 at.% of fluorine, F3. In fact, for coatings with higher fluorine contents, as the percentage of carbides decrease and the content in metallic fluorides increases, promoting a new change in structural and chemical composition, no cohesion failures were detected but the Lc_2 values were lower than the previous registered. This fact is related with the increase chemical disparity between the substrate and the coating as the fluorine content increases. As the chemical composition, structure and grain sizes vary from F0 to F7 sample it is difficult interpreting the results expecting a continuous variation of the critical loads with fluorine increase, due to the fact that more than one property varies from one sample to the next. Considering the characterization performed so far, the best coating for the envisaged application of modifying the surface of 316L vascular stents is F3.

The nanoindentation characterization allowed observing (Figures 5-8) that, in all tests, as the indentation depth increased the Young modulus of the samples diverged from the modulus of the coating to the substrates values (Hardness: $M_2=8.8\pm 0.30\text{GPa}$, $316L=4.76\pm 0.37\text{GPa}$; Young modulus: $M_2=200\pm 16\text{GPa}$, $316L=188\pm 12\text{GPa}$). The value of the divergence point varied from sample to sample due not only to the different chemical composition but also due to different thin film thickness as reported by other authors [7]. In fact, for samples F0 and F4 with similar thickness (Figures 5 and 7) this feature is observed for indentation depths higher than 84 nm, while for F6 coating (approximately 700 nm thick) (Figure 8) it is only visible at nearly 400 nm. It has been demonstrated that for oxide, oxynitride and fluoride glasses, the

Young modulus depends mainly of the chemical composition and the chemical bonding between atoms [29-31]. However, in this work almost all the 2D-FGC are nanocrystalline, unlike glasses which are amorphous. The contribution of the grain boundaries to the decrease of Young modulus when the grain size is lower than 30 nm has been reported [32]. On the coating without PTFE, F0 (Figure 5), the Young modulus is constant and similar to the bulk 316L. In fact, although the grain size is different the chemical compositions of the bulk and the deposited 316L are similar. The thin film with lower fluorine concentration, F1 (Figure 6), although with nanometric grain size, present an evolution of the Young modulus that can be attributed mainly to the chemical composition and chemical bonds. F4 coating (Figure 7) presents a more intense chemical gradient through the thickness of the film associated with the variation of the grain size from the substrate interface to the outmost layer (Figure 2b). This indicates that the evolution of the Young modulus values with increasing indentation depths can be influenced by both the chemical composition and the grain boundary effect. For the samples with higher fluorine content (Figure 8) the grain size dimensions imply a negligible contribution for the grain boundary effect. Thus, its behavior through the nanomechanical characterization is mainly due to the chemical composition.

The hardness, unlike the Young modulus, is more sensitive to the microstructure, as suggested by some deformation models of nanoindentation [33,34] and by the Hall-Petch relationship [35]. In 316L thin film (F0-Figure 5) the hardness is higher than the one of the bulk 316L which can be attributed to the smaller grain size [35]. The co-deposition at the lowest PTFE power density (Figure 6) does not bring any changes in the hardness evaluation. In fact, this result was expected as both the chemical composition and microstructure are very similar to F0 coating. Also, in both these systems, the evaluated mechanical properties are independent from the substrates as, for lower indentation depths, the values are very similar. However, the hardness analysis of the thin films with fluorine contents higher than 9 at.%

must also take in consideration the change of the structure from ferrite (bcc) to austenite (fcc) [3,4]. In fact, the appearance of the former crystallographic phase is mandatory for the envisaged application where the presence of magnetic properties is prohibited. The bcc structure is harder than the fcc which contributes to the slight decrease observed. Also the microstructural compatibility between the deposited thin films and the substrate is higher for 316L (fcc) than for M2 (bcc). This fact is highlighted by the small difference observed, even for low indentation depths, between the films deposited on the two substrates (Figure 8). For the highest fluorine contents the presence of higher concentrations of graphitic carbon is responsible for the hardness decrease.

In order to compare the hardness and Young modulus variation with the overall fluorine content of the deposited 2D-FGC the values at 0.7mN load were considered (Figure 9). This load allows comparing the results that incorporate the highest volume of the coating without the 316L substrate influence. The increase of the power density on the PTFE target, and consequent change from metallic to ionic chemical bonds is related to the decrease of the Young modulus. The hardness values can be divided in three zones according to Figure 9: I – major contribution of sputtered 316L bcc structure; II – contribution of fcc 316L structure and a decrease of the carbides presence; III – brittle ceramic compounds with the presence of graphitic carbon.

Conclusions

Co-sputtering of 316L stainless steel and PTFE allowed obtaining a chemical/structure gradient over the thickness of the deposited thin films. The nanoindentation of the coatings deposited on two steel substrates with different mechanical properties enable the determination of the indentation depth at which substrate influence become relevant, and thus distinguish it from the 2D-FGC value. After this preliminary study it was possible to select

the load value of 0.7 mN as appropriate to evaluate the mechanical properties of the deposited 2D-FGC, without substrate influence.

The increase in fluorine content induced a decrease in Young modulus from 180 to 80 GPa and a decrease of hardness from 8.5 to 6 GPa. For the highest fluorine concentration both Young modulus and hardness values decreases abruptly due to the presence of graphitic carbon.

Acknowledgements

This research is sponsored by FEDER funds through the program COMPETE (Programa Operacional Factores de Competitividade) and by national funds through FCT (Fundação para a Ciência e a Tecnologia), under the projects PEst-C/EME/UI0285/2013 and CENTRO-07-0224-FEDER-002001. J.Nunes also acknowledges FCT, Portugal, for the financial support through grant SFRH/BD/ 47586/ 2008. The authors gratefully acknowledge Prof. J.V.Fernandes for the fruitful scientific discussions.

References

- [1] S. Zhang, H.L. Wang, S. Ong, D. Sun, X.L. Bui, *Plasma Process. Polym.*, 4 (2007) 219-228.
- [2] H. Hassanin, K. Jiang, *Microelectron. Eng.*, 87 (2010) 1610-1613.
- [3] A.P. Piedade, J. Nunes, M.T. Vieira, *Acta Biomater.*, 4 (2008) 1073-1080.
- [4] A.P. Piedade, J. Nunes, M.T. Vieira, *J. Nanosci. Nanotechnol.*, 8 (2008) 1-6.
- [5] J. Nunes, A.P. Piedade, C.B. Duarte, M.T. Vieira, *Microsc. Microanal.*, 4(3) (2008) 35-36.
- [6] J.R. Roos, J.P. Celis, E. Vancoille, *Thin Solid Films*, 193/194 (1990) 547-556.

- [7] M. Wittling, A. Bendavid, P.J. Martin, M.V. Swain, *Thin Solid Films*, 270 (1995) 283-288.
- [8] J.V. Fernandes, L.F. Menezes, A.C. Trindade, *Thin Solid Films*, 335 (1998) 153-159.
- [9] J.V. Fernandes, A.C. Trindade, L.F. Menezes, A. Cavaleiro, *Surf. Coat. Tech.*, 131 (2000) 457-461.
- [10] A.M. Korsunski, A. Constantinescu, *Mater. Sci. Eng. A-Struct.*, 423 (2006) 28-35.
- [11] A. Tricoteaux, G. Duarte, D. Chicot, E. Le Bourhis, E. Bemporad, J. Lesage, *J. Mech. Mater.*, 42 (2010) 166-174.
- [12] C. Liu, R.G. Fairhurst, L. Renb, S.M. Greene, J. Tongb, R.D. Arnella, *Surf. Coat. Tech.*, 149 (2002) 143-150.
- [13] S.K. Mishra, P. Mahato, B. Mahato, L.C. Pathak, *Appl. Surf. Sci.*, 266 (2013) 209-213.
- [14] K.H.T. Raman, M.S.R.N. Kiran, U. G.M. Rao, *Appl. Surf. Sci.*, 258 (2012) 8629-8635.
- [15] F. Cai, S.H. Zhang, J.L. Li, Z. Chen, M.X. Li, L. Wang, *Appl. Surf. Sci.*, 258 (2011) 1819-1825.
- [16] K.S. Nakayama, Y. Yokoyama, G. Xie, Q.S. Zhang, M.W. Chen, T. Sakurai, A. Inoue, *Nano Lett.*, 8 (2008) 516-519.
- [17] L.M. López, O. Salas, L. Melo-Máximo, J. Oseguera, C.M. Lepienski, P. Soares, R.D. Torres, R.M. Souza, *Appl. Surf. Sci.*, 258 (2012) 7306-7313.
- [18] F. Jose F, R. Ramaseshan, A.K. Balamurungan, S. Dash, A.K. Tyagi, B. Raj, *Mat. Sci. Eng. A-Struct.*, 528 (2011) 6438-6444.
- [19] B. Song, P. Wu, S. Chen, S. Zhang, D. Yan, L. Xue, *Surf. Interface Anal.*, 44 (2012) 466-471.
- [20] S. Pathak, S.J. Vachhani, K.J. Jepsen, H.M. Goldman, S.R. Kalidindi, *J. Mech. Behav. Biomed. Mater.*, 13 (2012) 102-117.

- [21] T.J. Vaughan, C.T. McCarthy, L.M. McNamara, *J. Mech. Behav. Biomed. Mater.*, 12 (2012) 50-62.
- [22] C.F. Han, B.H. Wu, C.J. Chung, S.F. Chuang, W.L. Li, J.F. Lin, *J. Mech. Behav. Biomed. Mater.*, 12 (2012) 1-8.
- [23] B. Bar-On, H.D. Wagner, *J. Mech, Behav. Biomed. Mater.*, 12 (2012) 174-183.
- [24] J.M. Antunes, J.V. Fernandes, N.A. Sakharova, M.C. Oliveira, L.F. Menezes, *Int. J. Solids Struct.*, 44 (2007) 8313-8334.
- [25] J.M. Antunes, L.F. Menezes, J.V. Fernandes, *Int. J. Solids Struct.*, 44 (2007) 2732-2747.
- [26] D.R. Lide. *Handbook of Chemistry and Physics*, 85th ed. 2004, CRC Press, New York, section 5, pp. 5-25.
- [27] H. Keykamp, *J. Alloy Compd.*, 321 (2001) 138–145.
- [28] L. Ipaz, J.C. Caicedo, J. Esteve, F.J. Espinoza-Beltran, G. Zambrano, *Appl. Surf. Sci.*, 258 (2012) 3805-3814.
- [29] A. Makishima, J.D. Mackenzie, *J. Non-Cryst. Solids*, 12 (1973) 35-45.
- [30] M. Matecki, J. Lucas, *Mater. Res. Bull.*, 29 (1994) 473-477.
- [31] J. Rocherulle, C. Evolivet, M. Poulain, P. Verdier, U. Laurent, *J. Non-Cryst. Solids*, 108 (1989) 187-193.
- [32] Y. Zhou, U. Erb, K.T. Aust, G. Palumbo, *Scripta Mater.*, 48 (2003) 825-830.
- [33] M.L. Oyen, R.F. Cook, *J. Mech. Behav. Biomed. Mater.*, 2 (2009) 396-407.
- [34] G. Saada. *Mat. Sci. Eng.*, 400–401 (2005) 146-149.
- [35] Y.C. Lin, Y.J. Weng, D.J. Pen, H.C. Li, *Mater. Design* 30 (2009) 1643-1649.

Figure captions

Figure 1. Chemical gradient of sample F4 analyzed by XPS in-depth mode with indication of the analysis depth

Figure 2. Representative TEM bright field images and electron diffraction patterns of coatings: a) F1; b) F4 and c) F6

Figure 3. Schematic representation of the main compounds present in the deposited thin films: variation with fluorine content.

Figure 4. Optical micrographs of the scratch test (bar=20 μm). F1 at 70N (1a) and 20 N (1b); F3 at 70N (2a) and 50N (2b); F7 at 70N (3a) and 3N (3b).

Figure 5. Influence of indentation depth on F0 hardness and Young modulus values (open circles: M2 substrate; close circles: 316L substrate).

Figure 6. Influence of indentation depth on F1 hardness and Young modulus values (open circles: M2 substrate; close circles: 316L substrate).

Figure 7. Influence of indentation depth on F4 hardness and Young modulus values (open circles: M2 substrate; close circles: 316L substrate).

Figure 8. Influence of indentation depth on F6 hardness and Young modulus values (open circles: M2 substrate; close circles: 316L substrate).

Figure 9. Hardness (close squares) and Young modulus (open squares) as a function of the fluorine content, of the 2D-FGC deposited on 316L substrate, with 0.7mN load.

Table 1. XPS chemical composition, thickness and designation of the deposited thin films

Sample	PTFE power density (W.cm ⁻²)	Thickness (μm)	Chemical composition (at.%)						
			F	C	Fe	Cr	Ni	Mo	C/F
F0	0	0.5	0	7.3	57.4	26.7	7.0	1.6	--
F1	0.30	0.5	4.1	7.0	63.2	17.0	7.7	1.0	1.7
F2	0.40	0.6	5.7	8.7	63.0	13.9	7.7	1.0	1.5
F3	0.50	0.4	8.8	12.3	59.0	11.9	7.1	0.9	1.4
F4	0.60	0.4	18.8	20.6	35.8	9.6	4.1	1.1	0.7
F5	0.75	0.5	41.1	22.8	40.4	6.8	0.9	0.5	0.4
F6	0.95	0.7	47.7	23.7	20.7	4.5	2.9	0.6	0.5
F7	1.25	0.6	57.0	11.0	27.6	6.0	2.3	0.3	0.2

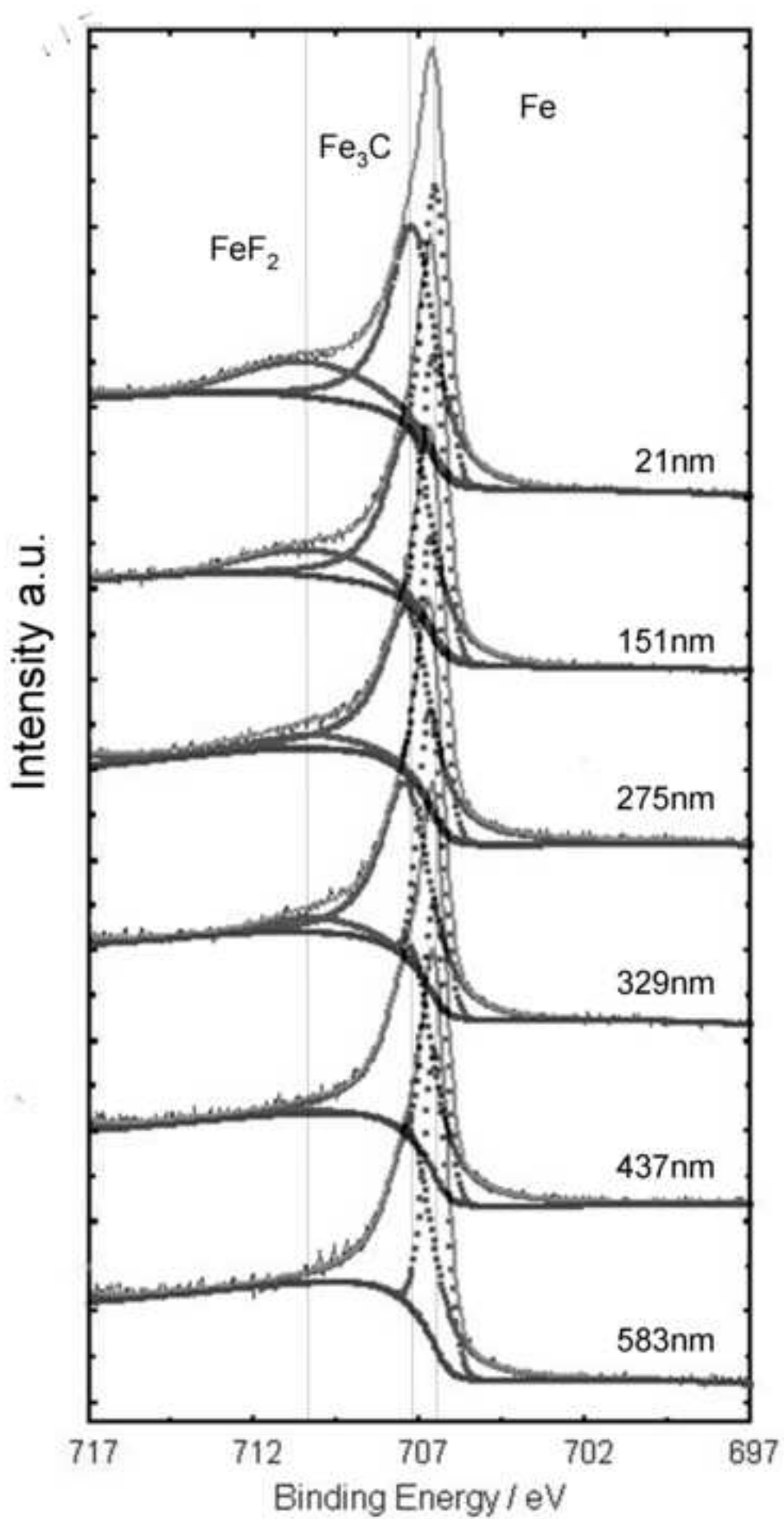
Table 2. Cohesive and adhesive failure values determined by scratch test.

Sample	LC1(N)		LC2(N)	
	mean	s.d.	mean	s.d
F0	68	1.8	>70	--
F1	n.d.	--	23	1.2
F2	n.d.	--	22	1.7
F3	56	3.2	>70	--
F4	n.d.	--	13	1.9
F5	n.d.	--	30	2.7
F6	n.d.	--	19	2.9
F7	n.d.	--	2	0.9

n.d. – not detected

- We produced functional graded coatings from steel and polymeric materials
- The gradation is both in chemical and structural composition through the thickness
- Nanoindentation of the coatings was made on two different steel substrates
- At 0.7 mN load the mechanical properties values converge

Accepted Manuscript



Manuscript

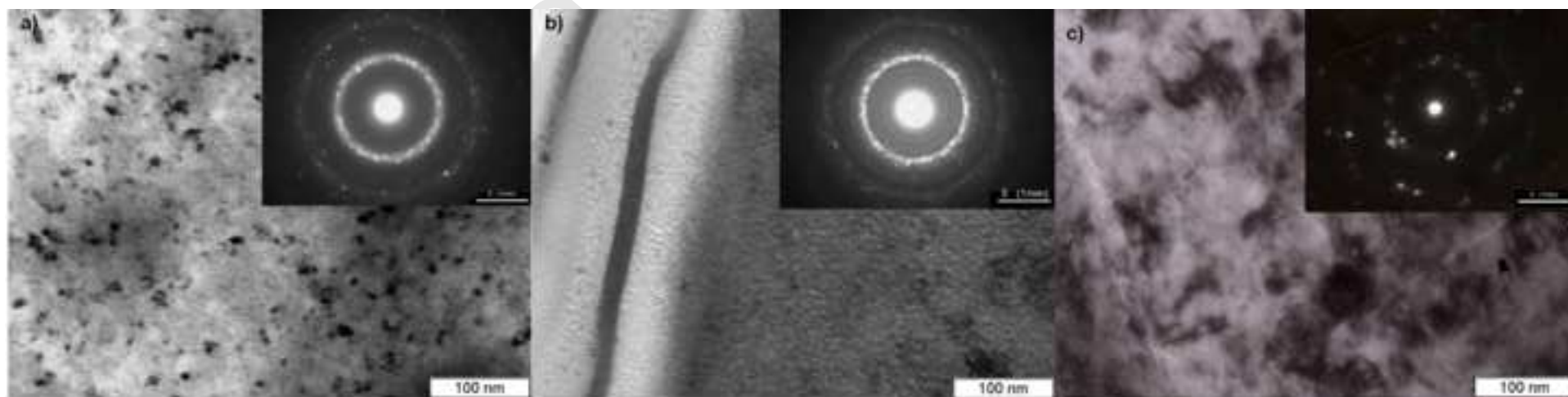


Figure 3

manuscript

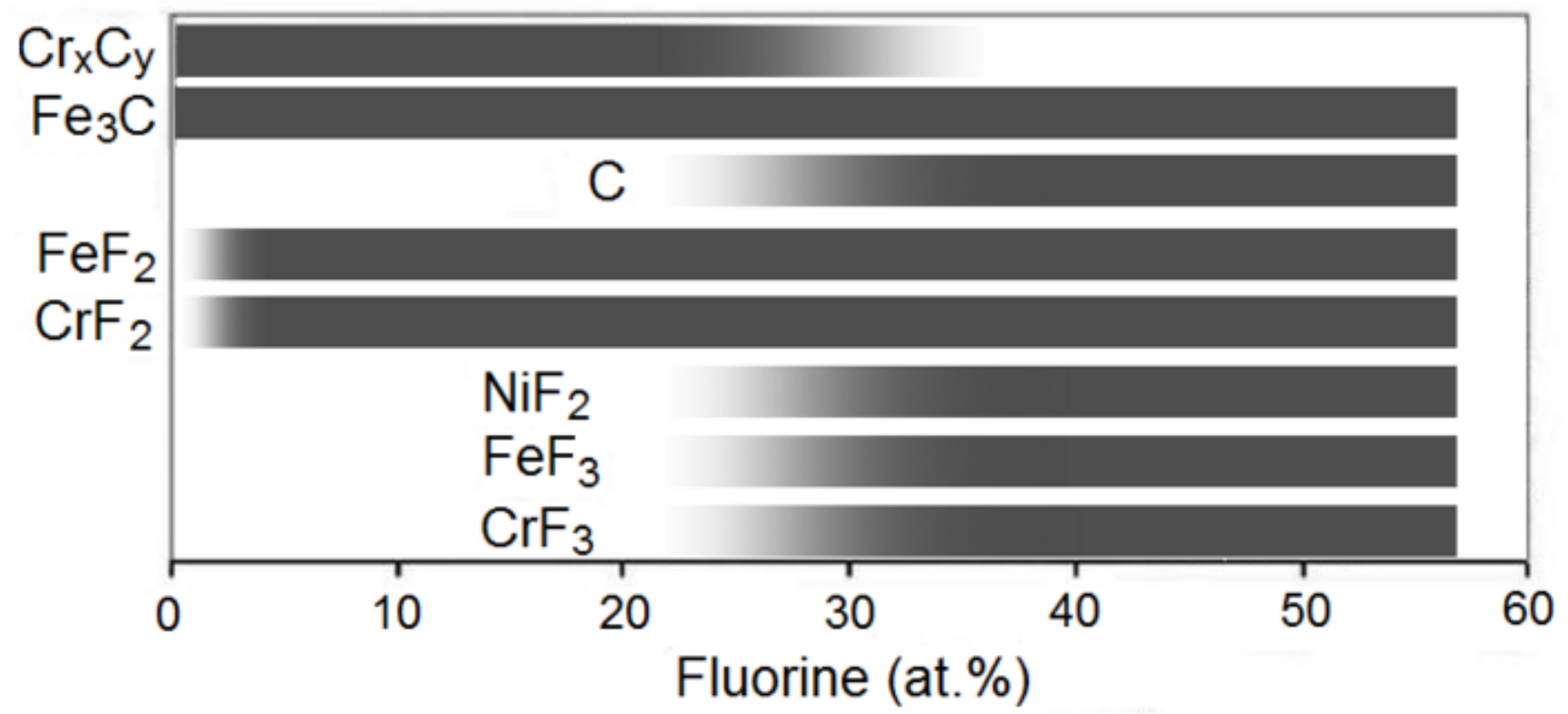
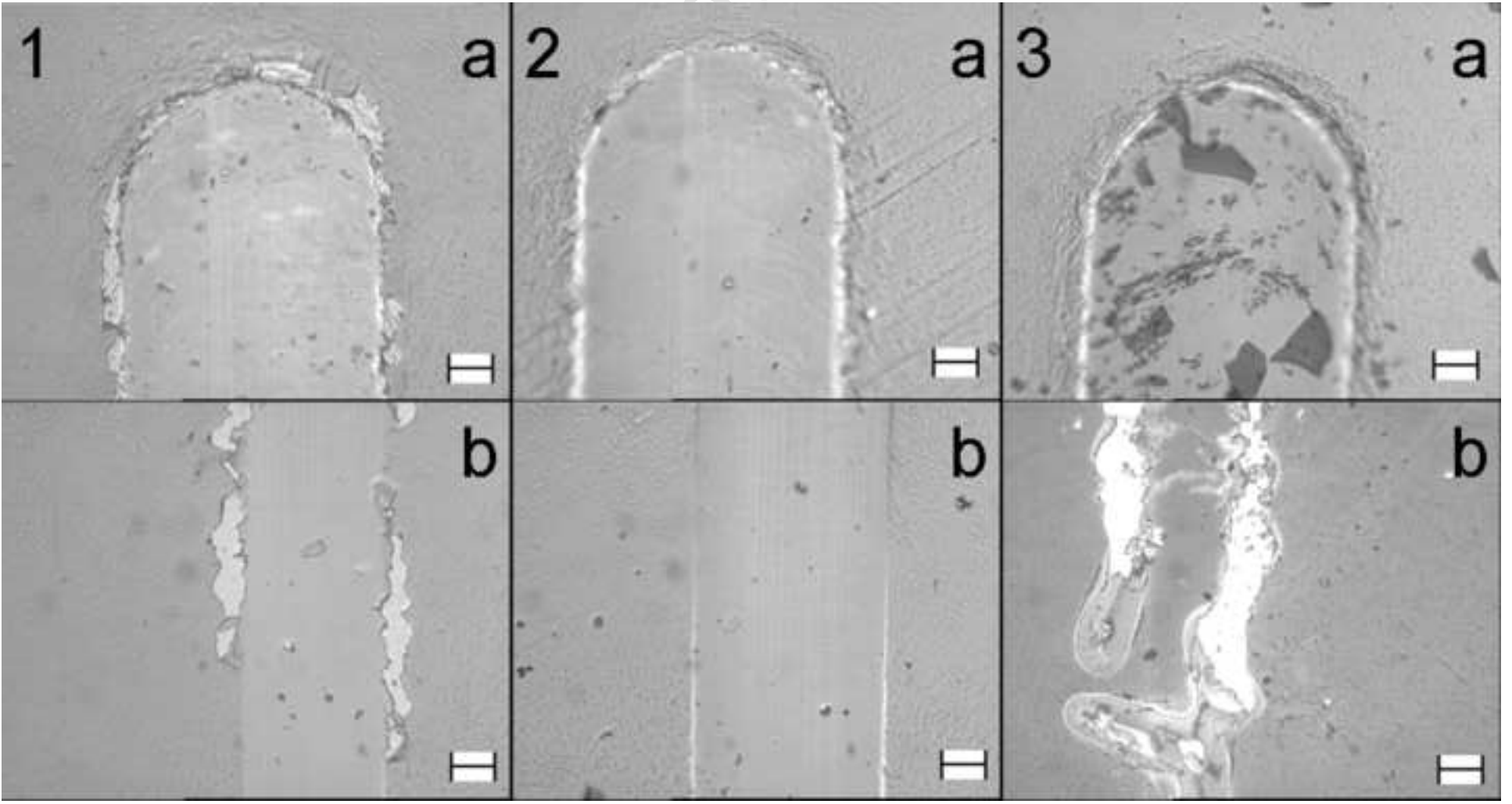
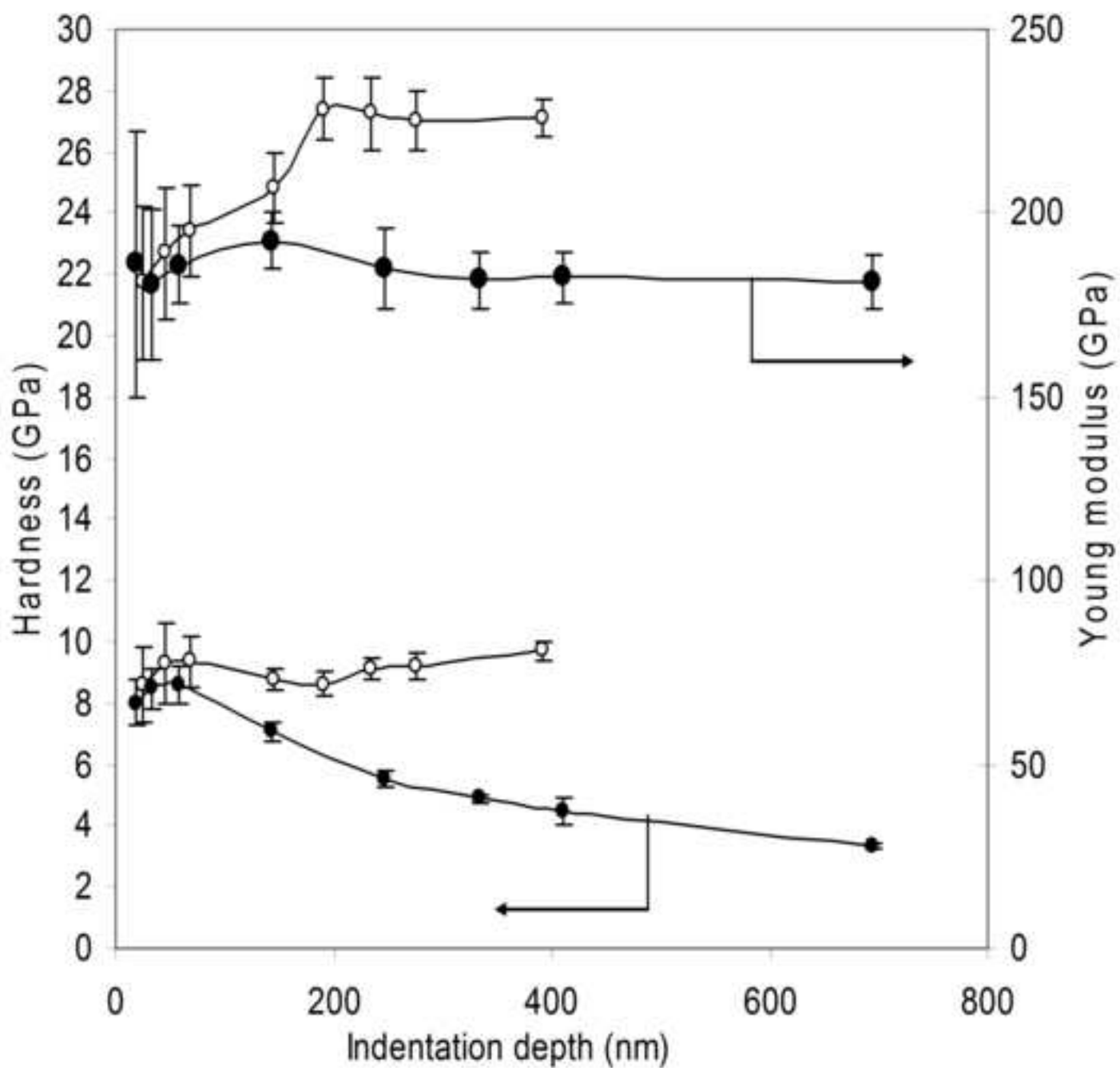
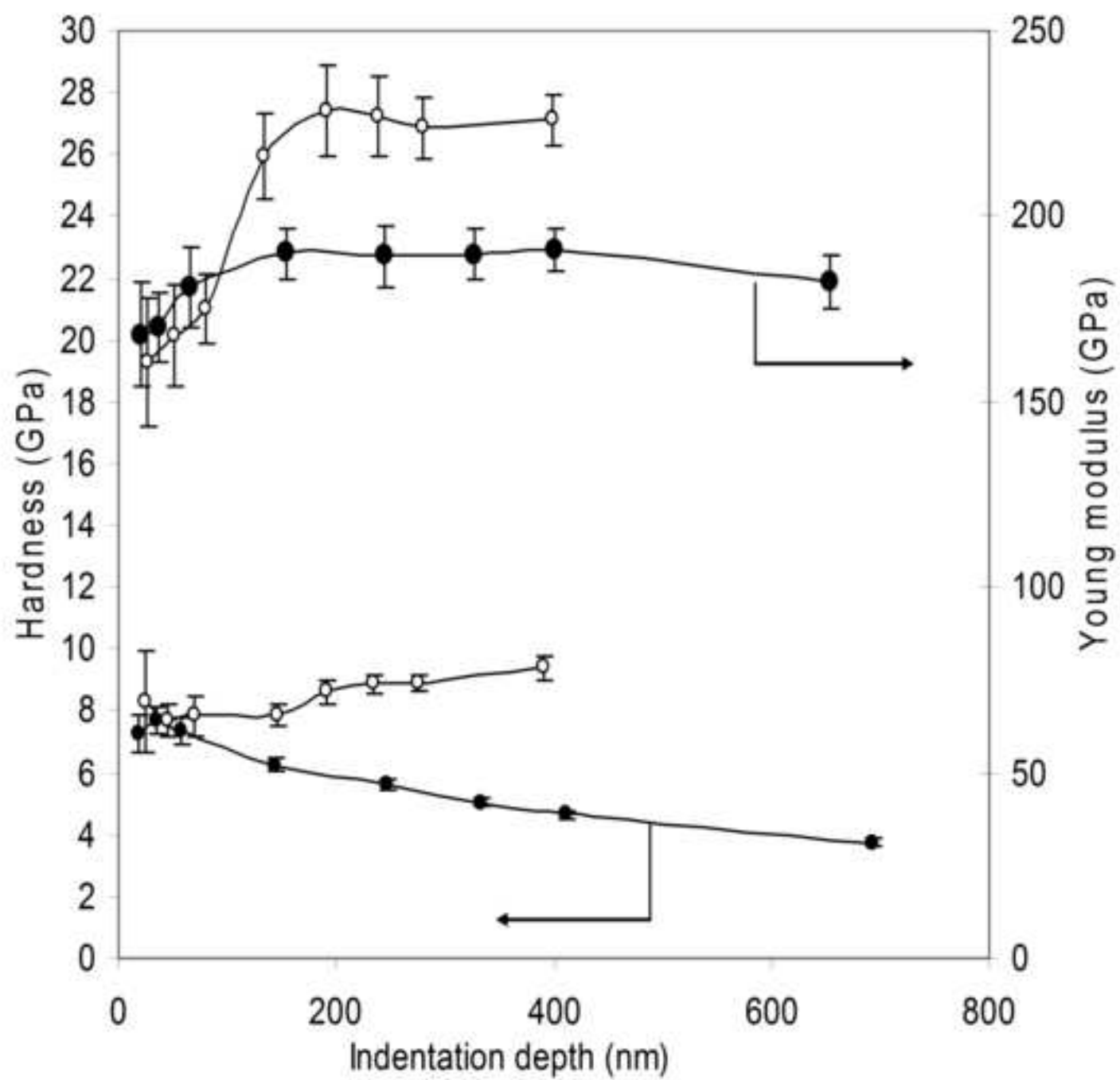
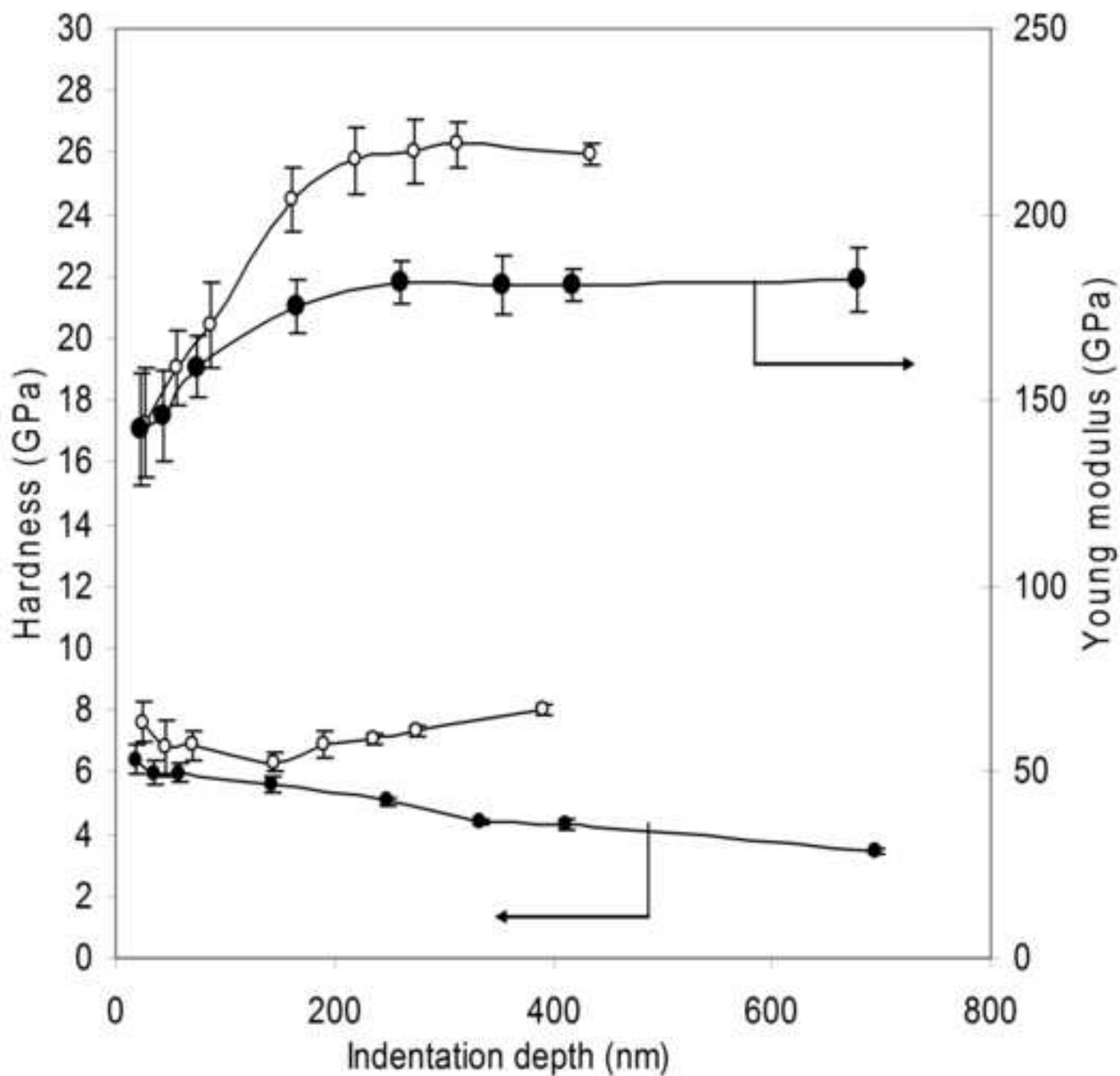


Figure 4









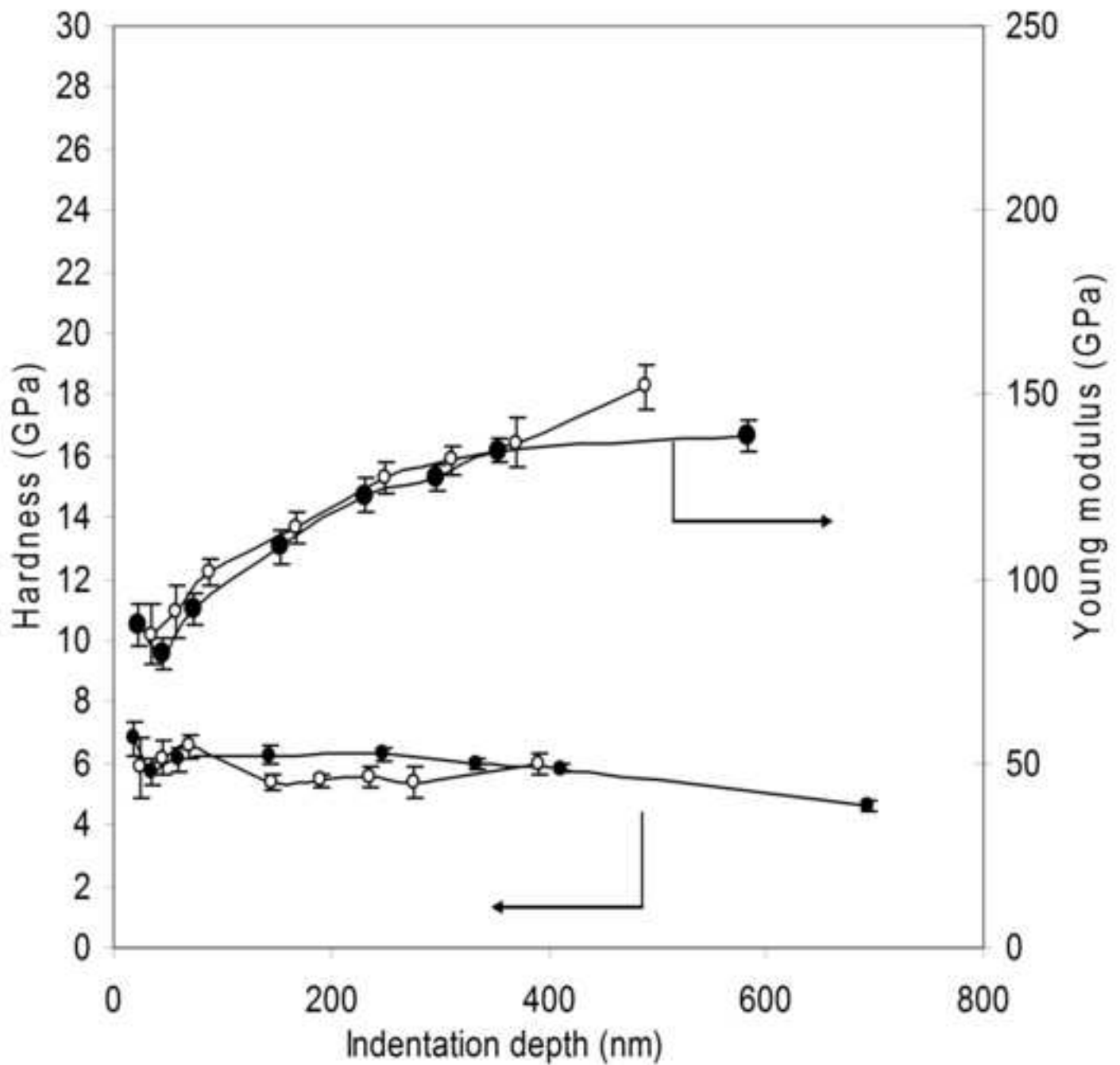


Figure 9

